Additive Weights for Straight Skeletons

Martin Held* Peter Palfrader*

Abstract

We introduce an *additively-weighted straight skeleton* as a new generalization of straight skeletons. It is induced by a wavefront propagation process where, unlike in standard variants, wavefront edges do not necessarily start to move at the begin of the propagation process but at later points in time.

1 Introduction

Straight skeletons were introduced to computational geometry over 20 years ago by Aichholzer et al. [2]. They have diverse applications such as in tool path generation, mathematical origami, roof design, and terrain generation. (See, for example, [7] and the references cited therein.)

The multiplicatively-weighted straight skeleton was first mentioned by Aichholzer and Aurenhammer [1] and then by Eppstein and Erickson [5]. Recently it was studied in more detail by Biedl et al. [3] who analyzed under which conditions properties of the unweighted skeleton carry over to the weighted pendant.

2 Preliminaries

A straight skeleton is defined as the outcome of a wavefront propagation process. For a simple polygon P, its wavefront $\mathcal{W}_P(t)$ changes with time t and is a set of simple polygons. Initially, at time zero, $\mathcal{W}_P(0)$ consists only of P. Then, as time increases, the edges of $\mathcal{W}_P(t)$ move towards the interior of P at unit speed in a self-parallel manner, preserving incidences. Thus, the vertices of $\mathcal{W}_P(t)$ move along the bisectors of polygon edges.

In order to maintain planarity of the wavefront during the propagation process, special processing is required to resolve non-planarities when they occur: In an *edge event*, an edge of the wavefront that has shrunk to zero length is removed. In a *split event*, a reflex vertex v reaches another part of the wavefront. The wavefront is split at this locus, and two separate polygons replace the previous polygon to restore planarity of the wavefront after the event. Typically this will happen when v reaches the interior of a wavefront edge. However, if v reaches another vertex then more complex interactions are possible [4]. The propagation process ends when all wavefront polygons have collapsed.

The traces of all vertices of $\mathcal{W}_P(t)$ over the propagation period then make up the edges of the straight skeleton $\mathcal{S}(P)$. In addition, if two parallel wavefront edges move into each other during the wavefront propagation, then the portion common to them is added to the straight skeleton while the portions that belong to only one of them remain in the wavefront [3].

To avoid ambiguities, we generally refer to the edges of the straight skeleton as *arcs* and reserve *edges* for the input polygon and the wavefront. Likewise, we call the vertices of the straight skeleton *nodes*.

The wavefront fragments of the polygon edge e at time t are contained in $\overline{e} + t \cdot n_e$, where $\overline{e}$ is the supporting line of e and n_e is its inward facing unit normal. We denote by $e(t)$ the (possibly empty) set of these wavefront fragments of edge e at time t. Every face of the straight skeleton is traced out by the fragments of exactly one input edge over time, i.e., $f(e) := \bigcup_{t \geq 0} e(t)$ for the face $f(e)$ of edge e.

Straight Skeletons with Multiplicative Weights. Multiplicatively-weighted straight skeletons, although introduced very early on, have been studied in detail only recently by Biedl et al. [3]. In the presence of multiplicative weights, wavefront edges no longer move at unit speed but instead move at different speeds depending on a weight function $\sigma\colon E \to \mathbb{R}$ where E is the edge-set of P. The wavefront fragments of the line e are contained in $\overline{e} + t \cdot \sigma(e) \cdot n_e$.

If all weights are required to be positive, then most of the well-known properties of straight skeletons are preserved. One prominent exception is that a face need not be monotone to its defining input edge any more. For negative weights, $\mathcal{S}(P)$ need not even be a tree and may contain crossings [3].

Please visit Held's CGA Lab [6] for references to prior work on straight skeletons and several examples.

3 Additively-Weighted Straight Skeletons

3.1 Definition

Given a simple polygon P and an additive-weight function $\delta\colon E \to \mathbb{R}_0^+$, we define the additively-weighted wavefront $\mathcal{W}_{P,\delta}(t)$ as follows. As in the unweighted case, $\mathcal{W}_{P,\delta}(0)$ is identical to P. However,

*Universität Salzburg, FB Computerwissenschaften, 5020 Salzburg, Austria; supported by Austrian Science Fund (FWF) Grant P25816-N15; {held,palfrader}@cosy.sbg.ac.at.

wavefront edges do not all start to move immediately. Rather, an edge of the wavefront that is emanated from polygon edge e will only start to move inwards at unit speed at time $\delta(e)$.

Since wavefront edges no longer move all at once, wavefront vertices will not travel exclusively along bisectors of input edges. If both incident wavefront edges have not yet started to move, then the wavefront vertex will obviously remain stationary. If exactly one incident wavefront edge has started to move, then the wavefront vertex will travel on the supporting line of the other; see Figure 2.

During its propagation process the wavefront will see instances of edge and split events, and it needs to be updated accordingly to restore planarity after the event. Note that even edges and vertices that have not yet started to move can be involved in both types of events. (See for instance the edge in the top right of Figure 1, which collapses before it starts moving.) The wavefront propagation process ends when all wavefront polygons have collapsed.

The *additively-weighted straight skeleton* $S(P, \delta)$ is then defined as the geometric graph whose edges are the traces of vertices of $\mathcal{W}_{P,\delta}(t)$ over its propagation period.

As in the unweighted case, we call edges of $S(P, \delta)$ *arcs* and its vertices *nodes*. Similarly, we again call the loci traced out by the wavefront segments $e(t)$ of edge e the *face* $f(e)$ *of* e, defined as $f(e) := \bigcup_{t \geq 0} e(t)$. We call the instance when an edge starts to move a *speed-change event*.

3.2 Properties

Node Degrees. In unweighted or multiplicatively-weighted straight skeletons, a node will be of degree one when it is a leaf of the straight skeleton (its locus will then be at a vertex of the input polygon) or of degree three when it is the result of an elementary edge or split event. Higher node degrees are also possible and are induced by non-elementary events where more than three wavefront edges are involved [4].

In addition to these types of nodes, the additively-weighted straight skeleton can have nodes of degree two. These occur when a vertex of the wavefront changes its speed due to an incident wavefront edge starting to move.

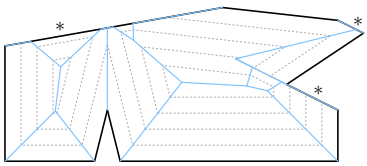

Figure 1: Polygon(black) with an additively-weighted straight skeleton (blue). The edges marked by $*$ have non-zero additive weights. A family of offset curves is shown in gray and dotted.

Nested Wavefronts. As in the case of unweighted or multiplicatively weighted straight skeletons with non-negative weights, the wavefronts of additively weighted straight skeletons are nested inside each other.

Lemma 1 *Let $t_1, t_2 \in \mathbb{R}_0^+$ with $t_1 < t_2$. Then $\mathcal{W}_{P,\delta}(t_2)$ lies within $\mathcal{W}_{P,\delta}(t_1)$.*

Proof. Edges that are already moving at time t_1 keep moving towards the interior of $\mathcal{W}_{P,\delta}(t_1)$. Edges that are still stationary do not move towards the outside either: Their incident vertices may move, however, as long as they stay on the same supporting line. As illustrated in Figure 2, these vertices do not move to the outside of the wavefront polygon either. □

Crossings, Planarity, and Connectedness. At time zero, the wavefront $\mathcal{W}_{P,\delta}(0)$ is a single simple polygon. Let t_1 be the earliest time at which an edge starts to move that was not moving initially, i.e., the time of the first non-trivial speed-change event. Then in the time interval $[0, t_1]$ the wavefront will propagate the same as if it were the wavefront of a multiplicatively-weighted polygon, where the weight of each edge is either 1 if it is already moving, or 0 if it is not yet moving.

Biedl et al. [3] show that the multiplicatively-weighted straight skeleton is free of crossings[1] for positive edge weights σ. This result extends to weights including zero. Therefore, the wavefront propagation in the time interval $[0, t_1]$ will not trace out any wavefront arcs that cross other arcs.

Now suppose that the wavefront propagation has not ended by time t_1. Then at time t_1 one or more edges will start to move and the wavefront $\mathcal{W}_{P,\delta}(t_1)$ will consist of one or more polygons. Lemma 1 implies that we can apply our reasoning to each wavefront polygon individually. If t_2 is the time of the next speed-change event, then by the same argument no wavefront arcs traced out during $[t_1, t_2]$ will cross either. Furthermore, arcs traced out during $[t_0, t_1]$ and $[t_1, t_2]$ will be confined to the areas that the wavefront traced out during their respective time. So no arc traced out during the latter interval can cross an arc traced out during the former. By induction, this claim holds for the entire wavefront propagation process.

Lemma 2 *The additively-weighted straight skeleton of a simple polygon is free of crossings.*

Note however, that we cannot infer strict planarity from being free of crossings: Assume v is a wavefront

[1] Roughly, a geometric graph G contains a crossing if there exists an arbitrarily small disk B centered on the interior of an arc such that no (open) half of B is empty of elements of the graph, or if two nodes of G share the same locus.

vertex where one incident edge e has not yet started to move. Let e' be the other edge incident at v. Then v travels on the supporting line of e, and the direction of this movement depends on the angle that e spans with e'; see Figure 2.

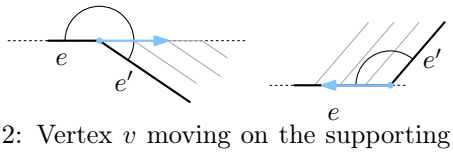

Figure 2: Vertex v moving on the supporting line of wavefront edge e that has not started to move yet.

Now let e' collapse in an edge event. Let e'' be the new neighbor of e and let v' be the new vertex that was created in this edge event. (At the time of the event, v' will be in the same locus as v, which it replaces in the wavefront.) If the angle at v' is now convex where at v it previously was reflex, then v' will move in the opposite direction of v. This results in the arc being traced out by v' to overlap the arc already traced out by v; see Figure 3.

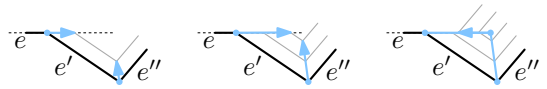

Figure 3: After an edge event, a wavefront vertex may backtrack along an arc previously traced out.

Lemma 3 *Let $\mathcal{S}_{P,\delta}(t)$ be the straight-skeleton features traced by the wavefront until time t. If two points $p, q \in \mathcal{S}_{P,\delta}(t)$ are path-connected on $\mathcal{S}_{P,\delta}(t) \cup \mathcal{W}_{P,\delta}(t)$, then they are path-connected on $\mathcal{S}(P,\delta)$.*

Proof. This is shown for multiplicatively-weighted straight skeletons in Lemma 13 of [3] by induction on the events of the wavefront propagation in chronological order. We know from their proof that connectivity of p and q is not broken by edge and split events. Therefore, it only remains to show that connectivity is maintained across speed-change events.

First, a speed-change event does not change the combinatorial properties of the wavefront. It will only result in vertices potentially moving at different speeds. Thus, a path between p and q cannot be split by changes to the wavefront.

Second, let us consider arcs being traced out by a vertex v of the wavefront. If v is not incident to a wavefront edge affected by a speed-change event at time t, it will just continue across the event with no change, tracing out a continuous arc. If, however, v is incident to an affected edge, then it will change direction, and therefore the arc that it traced out up until t will end at the position of v at time t. However, there it will connect via a node of degree two to the arc that v is tracing out after t. Thus, a path that goes over an arc currently being traced out by the wavefront cannot be disconnected by a speed-change event. □

Corollary 4 *The additively-weighted straight skeleton of a simple polygon is connected.*

Faces. For each edge e of P, we defined its face as $f(e) := \bigcup_{t\geq 0} e(t)$, where $e(t)$ is the set of segments of the wavefront at time t that were emanated by e. Initially, $e(0)$ will consist of only one segment that coincides with e, but as the wavefront propagates, segments may get split and segments may get dropped from $e(t)$ when they collapse. However, at no time will a segment just jump into existence. Hence each face is connected.

Note, however, that $f(e)$ is not necessarily a simple polygon for edges that do not immediately start to move. The faces in Figure 1 that correspond to the edges with non-zero additive weights demonstrate this fact. In clockwise order from the top left, we have a face whose interior is disconnected, a face with an empty interior because its corresponding edge collapsed before it started to move, and a face whose interior is not adjacent to e itself.

In the unweighted straight skeleton, the face of an edge e is a monotone polygon with respect to the supporting line of e. This is however not always the case for additively-weighted straight skeletons; see for example the topmost face in Figure 1.

Lemma 5 *A face of an additively-weighted straight skeleton need not be monotone with respect to the edge that emanated it.*

Roof Model. The roof model [2] raises the wavefront propagation into three-space, with the (third) z-coordinate being the time t. With P embedded in the $t = 0$ plane, the wavefronts over time thus form a polytope over P. This piecewise linear and continuous polytope $R(P) := \bigcup_{t\geq 0}(\mathcal{W}_P(t) \times \{t\})$ is called the *roof* of P. For unweighted straight skeletons the roof is a terrain (z-monotone).

The roof model is a useful theoretical tool when dealing with straight skeletons as it makes some proofs easier. It is also directly useful as a solution for modeling terrains or actual roofs of buildings.

The roof in the additively-weighted case is defined similarly as $R(P,\delta) := \bigcup_{t\geq 0}(\mathcal{W}_{P,\delta}(t) \times \{t\})$. It clearly is no longer strictly z-monotone, since wavefront edges may stay on the same supporting line during the propagation, resulting in vertical facets. The house depicted in Figure 4 has many such facets, namely the walls, as all input edges have (different) additive weights assigned to them. The weight assigned to some edges is larger, resulting in some walls continuing upwards while inclined roof facets already exist at the same height.

Lemma 6 *The roof $R(P,\delta)$ induced by an*

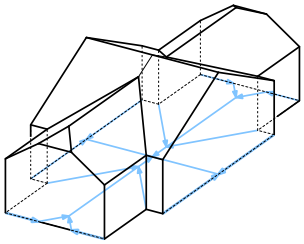

Figure 4: A house with a roof induced by an additively-weighted straight skeleton.

additively-weighted straight skeleton is weakly z-monotone.

Proof. This is a direct consequence of Lemma 1. □

For each edge e of the polygon, the roof will have at least one facet, the one incident to e. If the segments of e see a speed-change event during the propagation process, one additional facet per segment will be visible in the roof. Note that all facets of e correspond to only a single face in the straight skeleton as the "bend" caused by the speed-change event is not apparent in $\mathcal{S}(P, \delta)$. Also note that the total number of facets is still linear in the size of the input polygon since additional wavefront segments can only be caused by split events which are bounded linearly in the input size.

4 Generalizations

Several generalizations seem natural. First, one can combine multiplicative weights with additive weights. We postulate that no properties change as long as the multiplicative weights remain non-negative. If negative additive weights are allowed then the wavefront propagation would simply start at a time corresponding to the smallest negative weight. In terms of the roof model, negative weights merely mean shifting the whole structure along the z-axis.

Second, the additively-weighted straight skeleton can of course be defined not only for simple polygons but for planar straight-line graphs also.

Third, one could even allow more than a single speed-change per edge. As long as the speed function for an edge remains piecewise constant, vertices would still move along straight lines and the straight skeleton would be quite recognizable.

5 Computation

A simple method is described by Aichholzer et al. [2] to compute the unweighted straight skeleton: Compute the $\mathcal{O}(n)$ many collapse times of all edges and the $\mathcal{O}(n^2)$ times of all potential split events, and maintain them in a priority queue. On events, only a constant number of edge collapses have to be recomputed at constant cost each. Since the total number of events is linear, the overall algorithm runs in $\mathcal{O}(n^2 \log n)$ time at the cost of $\mathcal{O}(n^2)$ memory, where n is the size of the input polygon.

For the additively-weighted straight skeleton, the same approach can be used. The computation of potential split event times is slightly more involved but still in $\mathcal{O}(n^2)$. On speed-change events, a possibly linear number of collapses have to be recomputed, but the amortized cost for these is still only linear. Therefore, the additively-weighted straight skeleton can also be computed in $\mathcal{O}(n^2 \log n)$ time and $\mathcal{O}(n^2)$ space.

As in our prior work [8], we use a variant of Aichholzer and Aurenhammer's triangulation-based algorithm [1] for our implementation. Their core idea is to maintain a kinetic triangulation of the wavefront polygons, and keep track of triangle collapses in a priority queue as these signal events. We augmented the priority queue with the times of speed-change events, and are thus able to compute the additively-weighted straight skeleton.

Our implementation is based on CGAL and is capable of exactly computing the straight skeleton of a planar straight-line graph with non-negative additive and multiplicative weights. For instance, the straight skeletons and offsets in Figures 1 and 4 were produced by our code.

References

[1] O. Aichholzer and F. Aurenhammer. Straight Skeletons for General Polygonal Figures in the Plane. In *Voronoi's Impact on Modern Sciences II*, volume 21, pages 7–21. Institute of Mathematics of the National Academy of Sciences of Ukraine, 1998.

[2] O. Aichholzer, F. Aurenhammer, D. Alberts, and B. Gärtner. A Novel Type of Skeleton for Polygons. *J. Univ. Comp. Sci*, 1(12):752–761, 1995.

[3] T. Biedl, M. Held, S. Huber, D. Kaaser, and P. Palfrader. Weighted Straight Skeletons in the Plane. *Comp. Geom.: Theory and Appl.*, 48(2):120–133, Feb. 2015.

[4] T. Biedl, S. Huber, and P. Palfrader. Planar Matchings for Weighted Straight Skeletons. In *Proc. ISAAC*, pages 117–127, 2014.

[5] D. Eppstein and J. Erickson. Raising Roofs, Crashing Cycles, and Playing Pool: Applications of a Data Structure for Finding Pairwise Interactions. *Discrete & Comp. Geom.*, 22(4):569–592, 1999.

[6] M. Held. Weighted & Unweighted Straight Skeletons. `https://www.cosy.sbg.ac.at/~held/projects/wsk`.

[7] S. Huber. *Computing Straight Skeletons and Motorcycle Graphs: Theory and Practice.* Shaker Verlag, 2012.

[8] P. Palfrader, M. Held, and S. Huber. On Computing Straight Skeletons by Means of Kinetic Triangulations. In *Proc. ESA*, pages 766–777, 2012.